Available online at www.sciencedirect.com

ScienceDirect

www.elsevier.com/locate/jes

JES JOURNAL OF ENVIRONMENTAL SCIENCES

www.jesc.ac.cn

Heterogeneous reaction of NO_2 with feldspar, three clay minerals and Arizona Test Dust

Mingjin Tang[1,2,3], *Xiaohong Jia*[1,2], *Lanxiadi Chen*[1], *Wenjun Gu*[1], *Chengpeng Huang*[4], *Fu Wang*[4], *Lan Luo*[4], *Hongli Wang*[5], *Xinming Wang*[1], *Chao Peng*[1,*]

[1] *State Key Laboratory of Organic Geochemistry, Guangdong Key Laboratory of Environmental Protection and Resources Utilization, and Guangdong-Hong Kong-Macao Joint Laboratory for Environmental Pollution and Control, Guangzhou Institute of Geochemistry, Chinese Academy of Sciences, Guangzhou 510640, China*

[2] *CAS Center for Excellence in Deep Earth Science, Guangzhou 510640, China*

[3] *University of Chinese Academy of Sciences, Beijing 100049, China*

[4] *Longhua Center for Disease Control and Prevention of Shenzhen, Shenzhen 518109, China*

[5] *State Environmental Protection Key Laboratory of Formation and Prevention of Urban Air Pollution Complex, Shanghai Academy of Environmental Sciences, Shanghai 200233, China*

ARTICLE INFO

Article history:
Received 27 April 2022
Revised 12 July 2022
Accepted 13 July 2022
Available online 23 July 2022

Keywords:
Mineral dust
Heterogeneous reaction
Hygroscopicity
Mineralogy
Nitrogen oxides
Nitrate

ABSTRACT

Heterogeneous reaction of NO_2 with mineral dust aerosol may play important roles in troposphere chemistry, and has been investigated by a number of laboratory studies. However, the influence of mineralogy on this reaction has not been well understood, and its impact on aerosol hygroscopicity is not yet clear. This work investigated heterogeneous reactions of NO_2 (~10 ppmv) with K-feldspar, illite, kaolinite, montmorillonite and Arizona Test Dust (ATD) at room temperature as a function of relative humidity (<1% to 80%) and reaction time (up to 24 hr). Heterogeneous reactivity towards NO_2 was low for illite, kaolinite, montmorillonite and ATD, and uptake coefficients of NO_2, $\gamma(NO_2)$, were determined to be around or smaller than 1×10^{-8}; K-feldspar exhibited higher reactivity towards NO_2, and $CaCO_3$ is most reactive among the nine mineral dust samples considered in this and previous work. After heterogeneous reaction with NO_2 for 24 hr, increase in hygroscopicity was nearly insignificant for illite, kaolinite and montmorillonite, and small but significant for K-feldspar; in addition, large increase in hygroscopicity was observed for ATD, although the increase in hygroscopicity was still smaller than $CaCO_3$.

* Corresponding author.
E-mail: pengchao@gig.ac.cn (C. Peng).

https://doi.org/10.1016/j.jes.2022.07.023
1001-0742/

Introduction

Mineral dust, one of the most abundant components of aerosol particles in the troposphere (Ginoux et al., 2012; Textor et al., 2006; Wu et al., 2022), can significantly affect air quality (Ganor et al., 2009; Giannadaki et al., 2014; Zhang et al., 2013), radiation balance (Creamean et al., 2013; Karydis et al., 2011; Kok et al., 2018), and biogeochemical cycles of the Earth (Jickells et al., 2005; Mahowald et al., 2009). The frequency of Asian dust storms was high between 1950s and 1970s, and became much lower since then; Asian dust storms were very rare in the last decade, but several severe dust storms occurred in Asia in spring 2021 (Yin et al., 2021). After entrained into the troposphere, mineral dust can be transported over thousands of kilometers (Prospero and Mayol-Bracero, 2013; Uno et al., 2009) and undergo heterogeneous and multiphase reactions with various trace gases (Usher et al., 2003). These reactions can directly and indirectly affect abundance of a number of trace gases (Dentener et al., 1996; Tang et al., 2017; Usher et al., 2003) and also change composition of mineral dust particles (Laskin et al., 2005; Li and Shao, 2009; Sullivan et al., 2007), further modifying their physicochemical properties (Krueger et al., 2003; Shi et al., 2012; Sullivan et al., 2009a; Tang et al., 2016).

As an important reactive nitrogen species, NO_2 plays a central role in atmospheric chemistry (Seinfeld and Pandis, 2016), affecting the nitrogen cycle, tropospheric oxidation capacity, and formation of ozone and secondary aerosol. As a result, heterogeneous reaction of NO_2 with mineral dust particles has been investigated by a number of laboratory studies, as reviewed by Crowley et al. (2010). Nevertheless, large variations (up to two orders of magnitude) in the reported uptake coefficients, $\gamma(NO_2)$, have been found for different studies (Crowley et al., 2010; IUPAC, 2017), due to large uncertainties in estimating actual surface areas available for NO_2 uptake as well as the effects of mineralogy on heterogeneous reactivity. Mineralogy of dust aerosol is very complex (Journet et al., 2014; Nickovic et al., 2012; Scanza et al., 2015), and major minerals include quartz, clay minerals (such as illite, montmorillonite and kaolinite), feldspar, carbonate, and hematite. However, previous laboratory studies which investigated heterogeneous reaction of NO_2 with mineral dust are mainly focused on mineral oxides (such as SiO_2, Al_2O_3, Fe_2O_3 and TiO_2), carbonates and authentic mineral dust samples from different regions (Crowley et al., 2010). Uptake of NO_2 onto major clay minerals has been scarcely examined, and to our knowledge, heterogeneous reaction of NO_2 with feldspar, an important component in mineral dust, has never been investigated.

Laboratory studies (Krueger et al., 2003; Ma et al., 2012; Sullivan et al., 2009b; Tang et al., 2015; Vlasenko et al., 2006) suggest that heterogeneous uptake of acidic trace gases could increase hygroscopicity of mineral dust. For example, significant increase in hygroscopicity was observed for $CaCO_3$ particles after heterogeneous reaction with NO_2 (Jia et al., 2021; Liu et al., 2008), caused by the formation of highly hygroscopic $Ca(NO_3)_2$ (Gibson et al., 2006; Guo et al., 2019). Large increase in hygroscopicity were also observed in some studies for ambient mineral dust particles which contained Ca (or Mg) and might be aged carbonates particles (Laskin et al., 2005; Matsuki et al., 2005; Shi et al., 2008; Tobo et al., 2009); in contrast, some other field studies (Denjean et al., 2015; Massling et al., 2007) showed that hygroscopicity of mineral dust particles was not significantly increased after long-range transport. Therefore, one may speculate that among major minerals hygroscopicity would only be significantly enhanced for carbonates due to heterogeneous reaction with acidic gases. In fact, a few laboratory studies (Krueger et al., 2004; Ma et al., 2012) provided some clues for this speculation. For example, exposure to gaseous HNO_3 led to significant increase in hygroscopicity and change in morphology for carbonate particles, but changes in hygroscopic properties were negligible for quartz, aluminum silicate and gypsum (Krueger et al., 2004); moreover, another study (Ma et al., 2012) found that after heterogeneous reaction with gaseous acetic acid, increase in hygroscopicity was much smaller for Al_2O_3 than $CaCO_3$.

In this work, we investigated heterogeneous reactions of NO_2 (~10 ppmv) with K-feldspar, three clay minerals (illite, kaolinite and montmorillonite), and Arizona Test Dust as a function of relative humidity (RH, up to 80%) using a fixed-bed reactor, and measured changes in particle composition, hygroscopicity and Fe solubility after NO_2 uptake. Together with our previous studies which investigated heterogeneous reaction of NO_2 with iron oxides/hydroxides (Li et al., 2020) and $CaCO_3$ (Jia et al., 2021), this work aims to elucidate the effects of mineralogy on NO_2 uptake and thus to better assess the roles heterogeneous reaction of NO_2 with mineral dust plays in removal of nitrogen oxides and formation of nitrate aerosol. The second goal is to examine whether and to which extent NO_2 uptake can increase hygroscopicity of K-feldspar and clay minerals, thereby helping better understand hygroscopicity changes of mineral dust during transport in the troposphere.

1. Materials and methods

1.1. *Sample information*

In this work, five types of mineral dust samples were investigated, including K-feldspar, three clay minerals (illite, kaolinite and montmorillonite) and Arizona Test Dust (ATD), and all the samples were used without pretreatment. **Table 1** summarizes their sources, BET (Brunauer-Emmett-Teller) surface areas, and average particle diameters, as determined using methods described elsewhere (Chen et al., 2020; Tang et al., 2019b). Mineralogical compositions measured using X-ray diffraction are displayed in Appendix A Table S1 and Figure S1: no other minerals were detected for kaolinite and montmorillonite samples, and the illite sample was found to contain ~98% illite and ~2% kaolinite; the K-feldspar sample contained ~70% K-feldspar, ~26% Na-feldspar and ~4% quartz; the ATD sample contained ~49% quartz, ~15% K-feldspar, ~15% albite, ~11% illite, ~6% calcite and ~4% kaolinite.

1.2. *Heterogeneous interactions with NO_2*

The fixed-bed reactor used to investigate heterogeneous reaction of NO_2 with mineral dust is described elsewhere

Table 1 – Sources, BET surface areas, and average particle diameters of the five mineral dust samples.

Sample	Source	BET surface area (m^2/g)	Diameter (μm)
Illite	High Purity Clay Mineral Repository of China	35.76 ± 0.40	1.76 ± 0.02
Kaolinite	High Purity Clay Mineral Repository of China	24.09 ± 0.61	2.06 ± 0.10
Montmorillonite	High Purity Clay Mineral Repository of China	63.68 ± 0.63	16.75 ± 2.91
K-feldspar	National Research Center of Testing Techniques for Building Materials	3.96 ± 0.01	8.25 ± 1.57
ATD	Powder Technology Inc.	36.67 ± 1.06	1.05 ± 0.20

Note: Characterizations of K-feldspar and ATD were reported in our previous work (Chen et al., 2020).

(Jia et al., 2021; Li et al., 2020). In brief, a 200 mL/min mixed flow was passed through a particle-load polytetrafluoroethylene (PTFE) filter to start heterogeneous reaction of NO_2 with dust particles, and the PTFE filter (47 mm in diameter) was housed in a fluorinated ethylene propylene (FEP) filter holder. The mixed flow was generated by mixing a dry synthetic air flow, a humidified synthetic air flow and a NO_2 flow (1000 ppmv in synthetic air), which were regulated using three mass flow controllers. The NO_2 concentration in the mixed flow was set to 10 ± 0.5 ppmv (i.e., ~2.5×10^{14} molecule/cm^3), and the RH could be adjusted between <1% and 80%. After the mixed flow was passed through the filter, it was sampled by a T200 NO/NO_x analyzer (Teledyne Instruments, USA) to measure NO_2. Removal of NO_2 due to uptake onto mineral dust was very small, as changes in NO_2 concentrations were negligible when the mixed flow was passed through a particle-loaded filter (compared to a clean filter). Heterogeneous reactions were investigated in this work at room temperature (24 ± 2°C).

Mineral dust particles were loaded onto PTFE filters using the method described in our previous work (Jia et al., 2021; Li et al., 2020). Visual inspection suggested that mineral dust particles were relatively uniformly distributed on filters, and particle mass was determined to be 5 ± 1 mg for filter samples prepared in our work. If we assume that dust particles are spherical and their density is 2.7 g/cm^3, the number of layers of dust particles deposited on filters can be estimated with the knowledge of particle diameters (**Table 1**). The numbers of particle layers were estimated to be ~1.9 for ATD due to its smaller diameter (1.05 ± 0.20 μm on average) and 0.2-1.1 for the other four dust samples.

1.3. *Analysis*

A Q5000 vapor sorption analyzer (TA instruments, Delaware, USA), which measures sample mass change at different RHs to determine hygroscopic properties (Chen et al., 2020; Gu et al., 2017; Tang et al., 2019a), was used to measure hygroscopic properties of mineral dust samples before and after NO_2 uptake. This instrument was used in our previous study (Jia et al., 2021) to measure hygroscopic properties of fresh and aged $CaCO_3$ particles which were deposited onto PTFE filters, and the same experimental methodology was adopted in this work. In brief, the sample was first dried at < 1% RH, and then RH was stepwise increased to 80% by 20% per step; after that, RH was increased to 90%, and at last RH was changed to < 1% again. All the hygroscopicity measurements were conducted at 25°C, and at each step RH was changed to the next value only when the change in sample mass was < 0.05% in 60 min.

After hygroscopicity measurement, the particle-loaded filter was soaked in 10 mL deionized water and then stirred for 2 hr using an orbital shaker. The mixture was filtered through a polyethersulfone filter (0.22 μm pore size, Anpel, Shanghai, China), and the filtrate was then divided to two halves. The first half was analyzed using ion chromatography to determine the amount of nitrate (Jia et al., 2021), and the detection limit was 0.02 mg/L. The second half was acidified using 30 μL HNO_3 (67%-70% *V/V*, Optima Grade, Fisher Scientific) to contain 0.4% *V/V* HNO_3 for the final solution obtained, and the solution was then analyzed by inductively coupled plasma mass spectrometry to determine the amount of soluble Fe (Li et al., 2020).

1.4. *Uptake coefficients and surface coverages of formed nitrate*

The reaction uptake coefficient of NO_2, $\gamma(NO_2)$, defined as ratio of the reactive collision frequency to the total collision frequency, can be calculated using Eq. (1) (Jia et al., 2021; Li et al., 2010; Li et al., 2020):

$$\gamma(NO_2) = \frac{d[NO_3^-]}{dt}/Z \quad (1)$$

where the reactive collision frequency, $d[NO_3^-]/dt$, can be obtained from the average formation rate of nitrate due to NO_2 uptake. In this study, the average formation rate of nitrate in the first 3 hr was used to calculate initial $\gamma(NO_2)$. The total collision frequency (*Z*) between NO_2 molecules and particle surfaces can be determined using Eq. (2):

$$Z = \frac{1}{4} \times A_s \times [NO_2] \times c(NO_2) \quad (2)$$

where, A_s (cm^2) is the surface aera of mineral particles involved in heterogeneous reaction (equal to the BET surface area multiplied by the mass of particles on the filter), $[NO_2]$ (mol/cm^3) is the NO_2 concentration, and $c(NO_2)$ (cm/sec) is the mean molecular speed of NO_2.

The surface coverages (θ) of nitrate formed on the mineral under consideration can be calculated using Eq. (3) (Tang et al., 2016):

$$\theta = \frac{m(NO_3^-)}{m_0} \times \frac{N_A \cdot A(NO_3^-)}{M(NO_3^-) \cdot A_{BET}} \quad (3)$$

where, $m(NO_3^-)/m_0$ is defined as the mass ratio of nitrate to the initial mineral dust sample, N_A is the Avogadro constant

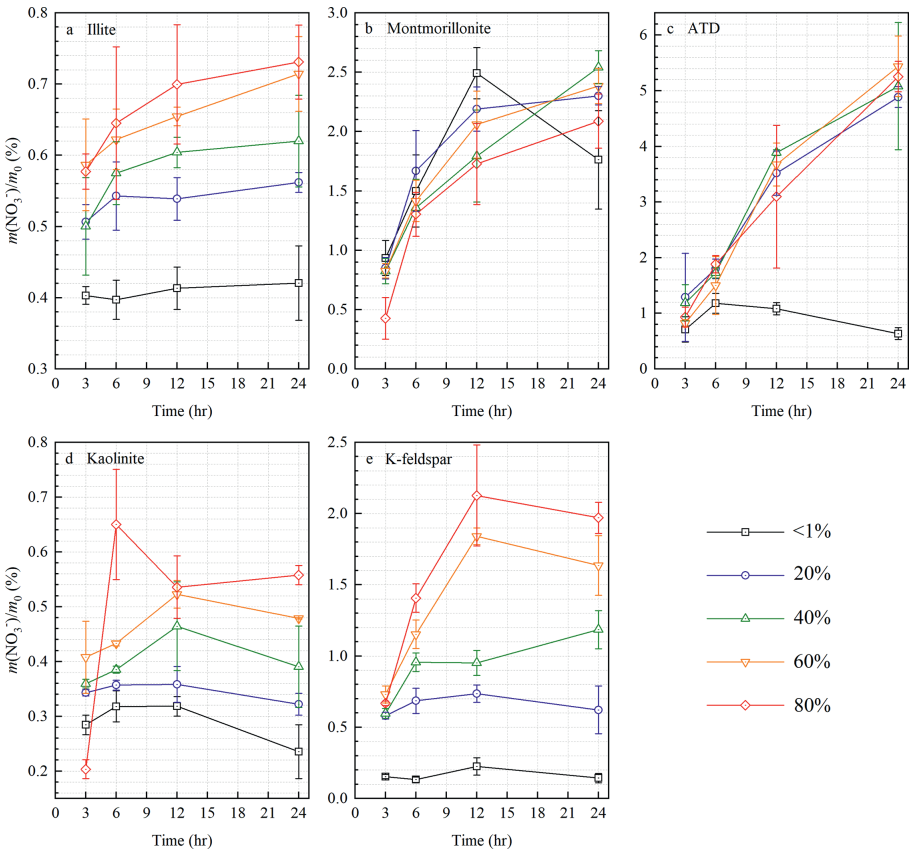

Fig. 1 – Mass fractions of nitrate which was formed due to heterogeneous reaction with 10 ppmv NO_2, $m(NO_3^-)/m_0$, as a function of time at different RHs. (a) illite, (b) montmorillonite, (c) ATD, (d) kaolinite, (e) K-feldspar.

(6.02×10^{23}/mol), $A(NO_3^-)$ is the average surface area of one nitrate ion (assumed to be 1×10^{-15} cm^2), $M(NO_3^-)$ (g/mol) is the molar mass of nitrate, and A_{BET} (m^2/g) is the BET surface area of the mineral under consideration.

2. Results and discussion

2.1. *Heterogeneous formation of nitrate*

The amounts of nitrate contained by mineral dust samples were measured prior to NO_2 uptake, and mass fractions of nitrate were found to be < 0.004% for all the five dust samples we examined. Fig. 1 shows changes in mass fractions of nitrate ($m(NO_3^-)/m_0$) formed due to heterogeneous reaction with 10 ppmv NO_2 as a function of time. It is evident that under dry conditions (< 1% RH) surface saturation was observed within 24 hr for all the five dust samples. For example, $m(NO_3^-)/m_0$ reached (0.40 ± 0.01)% at 3 hr and did not increase with further increase in reaction time for illite. Similarly, surface saturation was observed at 6 hr for ATD and kaolinite, and at 12 hr for montmorillonite and K-feldspar.

As shown in Fig. 1, the amounts of nitrate formed at elevated RH (20%-80%) were significantly larger than those at < 1% RH (except montmorillonite), suggesting the important effects of RH in heterogeneous reaction of NO_2 with mineral dust. Changes of formed nitrate with reaction time could be roughly classified into two categories for the five mineral dust samples examined in our work. For illite, montmorillonite and ATD, mass fractions of nitrate continuously increase with time (up to 24 hr), and thus their surfaces were not completely deactivated with respect to NO_2 uptake after 24 hr. In contrast, complete surface deactivation was observed for kaolinite and K-feldspar within 24 hr, and mass fractions of nitrate did not further increase with reaction time after 12 hr for the two minerals. In our previous work, under same/similar conditions surface saturation with respect to NO_2 uptake was observed for hematite and magnetite (Li et al., 2020) but not for goethite (Li et al., 2020) or $CaCO_3$ (Jia et al., 2021).

To further elucidate the effects of RH and mineralogy on nitrate formation, we compare the amounts of nitrate formed after reaction with 10 ppmv NO_2 for 24 hr at different RHs, and the results are summarized in Appendix A **Table S1** and **Fig. 2a**. As shown in **Fig. 2a**, overall three different RH dependences were observed: i) the amount of nitrate formed after 24 hr increased monotonously with RH (up to 80%) for illite, kaolinite and K-feldspar; ii) for montmorillonite, $m(NO_3^-)/m_0$ first increased with RH (<1% to 40%) and then decreased with further increase in RH (40% to 80%); iii) similar to $CaCO_3$ examined in our previous work (Jia et al., 2021), increase in RH from < 1% to 20% led to large enhancement in nitrate formation for ATD, and further increase in RH up to 80% did not have significant effects.

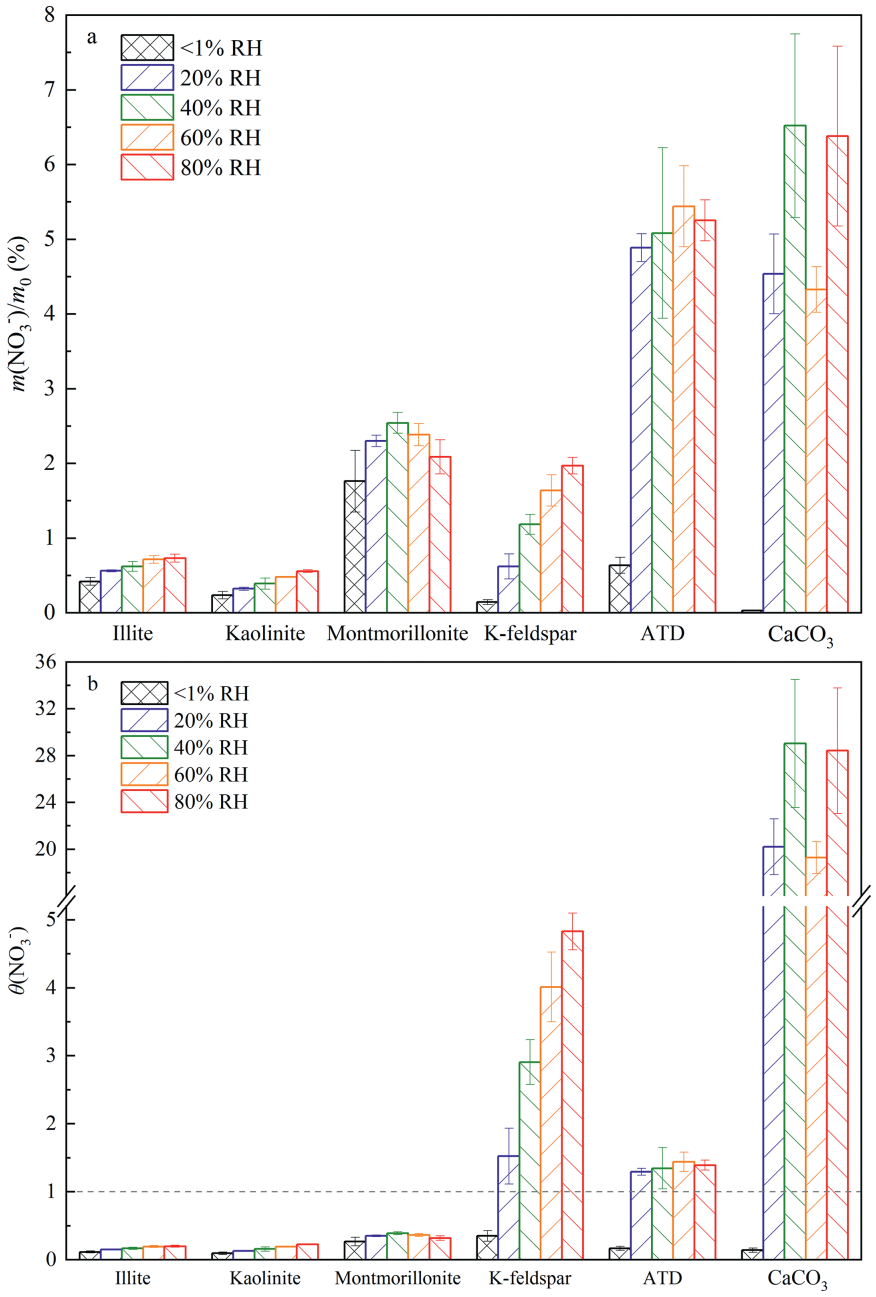

Fig. 2 – The amounts of nitrate formed on different mineral dust samples after heterogeneous reaction with 10 ppmv NO_2 for 24 hr at different RHs. (a) $m(NO_3^-)/m_0$, mass ratios of nitrate to the initial mineral dust, (b) $\theta(NO_3^-)$, surface coverages of nitrate. Reaction of NO_2 with $CaCO_3$ was examined in a previous study (Jia et al., 2021).

Fig. 2a and Appendix A Table S1 also reveal large variations in the amount of formed nitrate for different minerals. Mass fractions of formed nitrate after reaction with 10 ppmv NO_2 for 24 hr were always <1% for illite and kaolinite; for comparison, more nitrate was formed for K-feldspar and montmorillonite, and mass fractions of nitrate could reach ~2% for K-feldspar and ~2.5% for montmorillonite. Much more nitrate was formed for ATD and $CaCO_3$, and mass fractions of nitrate reached ~5%.

Mass fractions of nitrate could be converted to its surface coverages, assuming that each nitrate ion occupies an area of 1×10^{-15} cm^2 on the surface (Li et al., 2020; Tang et al., 2016), and the results can be found in **Fig. 2b and Appendix A Table S2**. After reaction with 10 ppmv NO_2 for 24 hr, surface coverages of nitrate were < 1 for illite, kaolinite and montmorillonite, probably implying that not all the surface sites are reactive towards NO_2 for the three clay minerals; on the contrary, surface coverages of nitrate increased from ~0.4 at <1% RH to ~4.8 at 80% RH for K-feldspar. Furthermore, surface coverages of nitrate were low (< 0.2) for ATD and $CaCO_3$ at < 1% RH and were substantially increased at elevated RH (20%-80%). As shown in **Fig. 2**, although mass fractions of formed nitrate

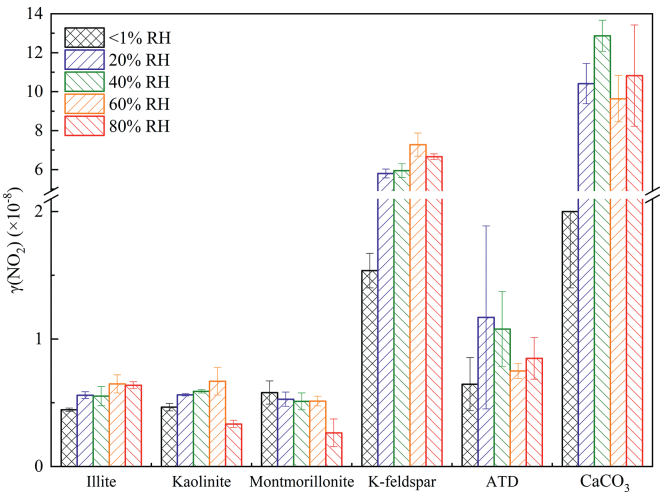

Fig. 3 – Average uptake coefficients in the first three hours for heterogeneous reaction of NO_2 (10 ± 0.5 ppmv) with different minerals at different RHs. Uptake coefficients of NO_2 onto $CaCO_3$ were reported in our previous work (Jia et al., 2021).

were similar for ATD and $CaCO_3$ at 20%-80% RH, surface coverages of nitrate were significantly smaller for ATD, and the reason is that the BET surface area of ATD (36.67 m^2/g) is much larger than $CaCO_3$ (2.18 m^2/g).

In addition, we also examined iron solubility of the five dust samples before and after uptake of NO_2 at different RHs. It was found that after reaction with NO_2 (10 ppmv) for 24 hr, changes in Fe solubility were insignificant for all the five dust samples.

2.2. *Uptake coefficients*

2.2.1. *Effects of RH and mineralogy*

As described in our previous work (Jia et al., 2021; Li et al., 2020), the average nitrate formation rates in the first three hours, are used to calculate uptake coefficients of NO_2, $\gamma(NO_2)$, and it is assumed in our calculation that the surface area available for NO_2 uptake was equal to the BET surface area of the dust sample (m^2/g) multiplied by its mass on the filter (~5 mg).

As displayed in **Fig. 3**, the effects of RH on $\gamma(NO_2)$ showed different features for the five minerals investigated. Among the three clay minerals, $\gamma(NO_2)$ showed a slightly positive dependence on RH for illite, increasing from ~4.4×10^{-9} at < 1% RH to 6.4×10^{-9} at 80% RH; $\gamma(NO_2)$ first increased slightly with RH from 4.7×10^{-9} at <1% RH to 6.7×10^{-9} at 60% RH for kaolinite, and then decreased remarkably to 3.3×10^{-9} at 80% RH; in addition, $\gamma(NO_2)$ decreased with RH from 5.8×10^{-9} at <1% RH to 2.6×10^{-9} at 80% RH for montmorillonite. No apparent dependence of $\gamma(NO_2)$ on RH was observed for ATD over the entire RH range (<1% to 80%) if the experimental uncertainties were considered. For K-feldspar, $\gamma(NO_2)$ increased from 1.54×10^{-9} at < 1% RH to 5.80×10^{-9} at < 20% RH, but further increase in RH (up to 80%) did not lead to significant change in $\gamma(NO_2)$; as shown in **Fig. 3**, similar RH dependence of $\gamma(NO_2)$ was also observed for $CaCO_3$ in our previous study (Jia et al., 2021).

Table 2 summarizes $\gamma(NO_2)$ for the five mineral dust samples determined in this work, to compare with those for $CaCO_3$ (Jia et al., 2021) as well as hematite, magnetite and goethite (Li et al., 2020). At elevated RH (20%-80%) which are more relevant for the troposphere, surfaces of the three clay minerals and ATD show very low reactivity towards NO_2, and their $\gamma(NO_2)$ values are around or smaller than 1×10^{-8}; the other five mineral dust samples exhibit higher reactivity, and their $\gamma(NO_2)$ values can be described by the following order: $CaCO_3$ > K-feldspar > goethite > magnetite > hematite. The IUPAC Task Group on Atmospheric Chemical Kinetic Data Evaluation reviewed laboratory work which investigated heterogeneous reaction of mineral dust with NO_2, and a preferred value of 9×10^{-9}, measured for Saharan dust which is an authentic dust sample (Ndour et al., 2009), has been recommended with an estimated uncertainty of a factor of 10 (IUPAC, 2017). The recommended value is consistent with $\gamma(NO_2)$ determined in our work for ATD, which is also an authentic dust sample. Therefore, a value of 1×10^{-8}, which is essentially equivalent to 9×10^{-9} preferred by the IUPAC Task Group on Atmospheric Chemical Kinetic Data Evaluation (IUPAC, 2017), is recommended to assess atmospheric significance of heterogeneous reaction of NO_2 with mineral dust aerosol.

2.2.2. *Comparison with previous studies*

Zhang et al. (2012) investigated heterogeneous reaction of NO_2 (9×10^{14}-25×10^{14} molecule/cm^3) at different RHs (< 1%-80%) with montmorillonite using diffuse reflectance infrared Fourier transform spectroscopy (DRIFTS), and $\gamma(NO_2)$ were determined to be in the range of (3.6-11) $\times 10^{-9}$ for Na-montmorillonite and (5.7-10.5) $\times 10^{-9}$ for Ca-montmorillonite (Appendix A **Table S3**); the results reported by Zhang et al. (2012) are broadly consistent with $\gamma(NO_2)$ values determined in our present work (2.6×10^{-9} to 5.8×10^{-9}). Three previous studies (Angelini et al., 2007; Liu et al., 2015; Zhang et al., 2011) investigated NO_2 uptake onto kaolinite, and their experimental conditions and uptake coefficient results are summarized in Appendix A **Table S3**. The $\gamma(NO_2)$ values were found to be in the range of 8.1×10^{-8} to 2.3×10^{-7} under dry conditions (<1% RH) by Angelini et al. (2007), increasing with NO_2 concentrations (0.56×10^{13} to 8.8×10^{13} molecule/cm^3); in addition, $\gamma(NO_2)$ were determined to be in

Table 2 – Comparison of $\gamma(NO_2)$ (x 10^{-8}) for different mineral dust samples.

Sample	< 1% RH	20% RH	40% RH	60% RH	80% RH
Illite	0.44 ± 0.01	0.56 ± 0.03	0.55 ± 0.08	0.65 ± 0.07	0.64 ± 0.03
Kaolinite	0.47 ± 0.03	0.56 ± 0.01	0.59 ± 0.01	0.67 ± 0.11	0.33 ± 0.03
Montmorillonite	0.58 ± 0.09	0.53 ± 0.06	0.51 ± 0.07	0.51 ± 0.04	0.26 ± 0.11
K-feldspar	1.54 ± 0.14	5.80 ± 0.23	5.95 ± 0.35	7.28 ± 0.60	6.66 ± 0.15
ATD	0.65 ± 0.21	1.17 ± 0.72	1.08 ± 0.30	0.75 ± 0.06	0.85 ± 0.16
$CaCO_3$	2.00 ± 0.60	10.41 ± 1.04	12.87 ± 0.80	9.64 ± 1.19	10.82 ± 2.60
Hematite[a]	1.09 ± 0.15	1.35 ± 0.22 [b]		1.20 ± 0.48	1.21 ± 0.38 [c]
Magnetite[a]		2.91 ± 0.42 [b]		2.70 ± 0.60	
Goethite[a]		4.83 ± 0.94 [b]		4.03 ± 0.32	

The $\gamma(NO_2)$ values for hematite, magnetite, goethite and $CaCO_3$ were reported in our previous work (Jia et al., 2021; Li et al., 2020).
[a] $[NO_2] = 2.5 \pm 0.1$ ppmv
[b] at 30% RH
[c] at 90% RH.

the range of (1.3-4.0) × 10^{-8} by Zhang et al. (2011) and (3.1-14.4) × 10^{-8} by Liu et al. (2015). Despite different techniques were employed, $\gamma(NO_2)$ values for kaolinite reported by the previous three studies (Angelini et al., 2007; Liu et al., 2015; Zhang et al., 2011) agreed well with each other, but were approximately 1-2 orders of magnitude larger than those obtained in our work. As shown in Appendix A **Table S3**, $\gamma(NO_2)$ was determined to be ~1 × 10^{-9} at 25% RH for ATD particles by Ndour et al. (2008), about one order of magnitude smaller than our results (6.5 × 10^{-9} to 11.7 × 10^{-9}). To our knowledge, heterogeneous reaction of NO_2 with feldspar has not been examined before.

Large uncertainties in uptake coefficients for heterogeneous reactions with mineral dust stem mainly from large errors in estimating actual surface areas of dust particles available for heterogeneous uptake when multiple layers of dust particles are used (Crowley et al., 2010; Tang et al., 2017), and surface areas estimated using different methods and thus uptake coefficients reported can vary by a few orders of magnitude. The number of layers of particles deposited on PTFE filters was < 2 in our work, and most of these particles should be available for NO_2 uptake, thereby substantially reducing the uncertainties in estimating surface areas available for NO_2 uptake. As a result, we believe that $\gamma(NO_2)$ reported in our work are more reliable than those reported in previous studies (Angelini et al., 2007; Dupart et al., 2014Liu et al., 2015; Ndour et al., 2008, 2009; Zhang et al., 2012; Zhang et al., 2011) in which multiple layers of dust particles were used.

2.3. *Change in hygroscopicity*

Fig. 4a displays time series of RH and m_w/m_0 (the relative mass of adsorbed water, defined as the mass ratio of adsorbed water as a given RH to the initial mineral dust sample at < 1% RH) for an ATD sample after reaction with 10 ppmv NO_2 for 24 hr at 80% RH, and the data displayed in **Fig. 4a** can be used to derive m_w/m_0 as a function of RH. **Fig. 4b** displays m_w/m_0 for ATD particles before and after heterogeneous reaction with NO_2. It is evident that m_w/m_0 at 90% RH was significantly larger for aged ATD (~0.239) than fresh ATD (~0.058). This suggests that after heterogeneous reaction with 10 ppmv NO_2 for 24 hr at 80% RH, hygroscopicity of ATD particles was significantly increased.

To further explore impacts of NO_2 uptake on hygroscopic properties of mineral dust, we focus our discussion on hygroscopicity of fresh and aged dust particles at 90% RH, represented by $m_w(90\%)/m_0$. **Fig. 5** displays $m_w(90\%)/m_0$ for the five mineral dust samples before and after heterogeneous reaction with NO_2, and hygroscopicity of fresh and aged $CaCO_3$ particles, measured in previous work (Jia et al., 2021), is also included for comparison. In addition, these results are summarized in Appendix A **Table S4**. All the mineral dust samples were aged under the same condition (10 ppmv NO_2, 24 hr), but RH (<1%, 20%, 40%, 60% or 80%) was varied in individual uptake experiments.

As shown in **Fig. 5** and Appendix A **Table S4**, changes in hygroscopicity varied substantially for the six mineral dust samples. Increase in hygroscopicity due to NO_2 uptake was insignificant for montmorillonite, because the hygroscopicity of fresh montmorillonite was high ($m_w(90\%)/m_0$: ~0.24) and the amount of nitrate formed was quite limited ($m(NO_3^-)/m_0$: <3%); furthermore, the increase in hygroscopicity after heterogeneous reaction with NO_2 was minor or even insignificant for the other two clay minerals (illite and kaolinite), due to very limited amounts of nitrate formed ($m(NO_3^-)/m_0$: <1%). In addition, small but significant enhancement in hygroscopicity was in general observed for K-feldspar after NO_2 uptake, and the extent of hygroscopicity increased with RH at which NO_2 uptake took place. For example, hygroscopicity was not increased for K-feldspar after reaction with NO_2 at <1% RH; however, $m_w(90\%)/m_0$ was increased significantly from ~0.005 to ~0.094 for K-feldspar after NO_2 uptake at 80% RH.

Fig. 5 further reveals that large enhancement in hygroscopicity, due to NO_2 uptake, was observed for ATD, similar to $CaCO_3$ examined previously (Jia et al., 2021). However, increase in hygroscopicity was larger for $CaCO_3$ (compared to ATD) when NO_2 uptake occurred at elevated RH (20%-80%). This is probably because in addition to carbonates, ATD also contains substantial amount of other minerals (such as clays, feldspar and quartz) for which the increase in hygroscopicity is not so substantial as $CaCO_3$ after heterogeneous reaction with NO_2.

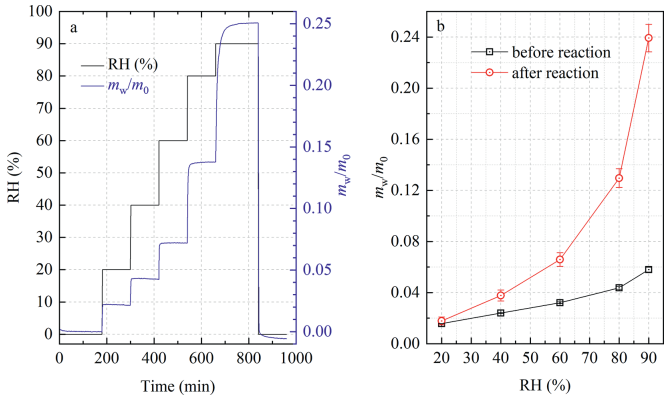

Fig. 4 – (a) Changes in RH and relative mass of absorbed water (m_w/m_0, defined as the mass ratio of adsorbed water at a given RH to the initial mineral dust sample at <1% RH) with time for an aged ATD sample, (b) m_w/m_0 as a function of RH for fresh and aged ATD particles. The aged sample displayed in this figure is an ATD sample after heterogeneous reaction with 10 ppmv NO_2 for 24 hr at 80% RH.

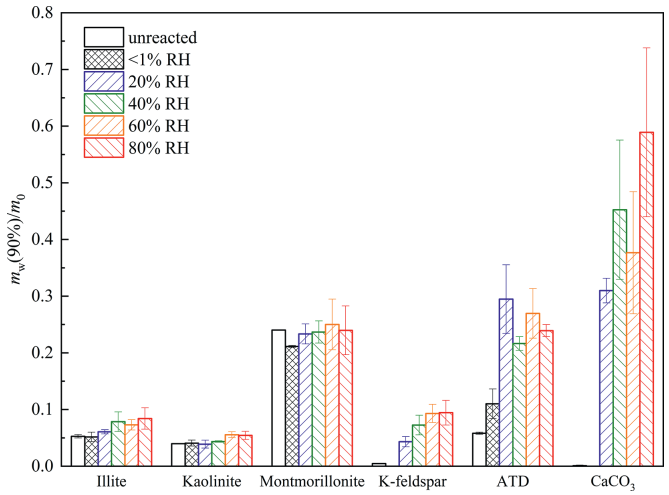

Fig. 5 – Hygroscopicity at 90% RH, represented by $m_w(90\%)/m_0$, for different mineral dust particles before and after heterogeneous reaction with 10 ppmv NO_2 for 24 hr at different RHs. Changes in hygroscopicity of $CaCO_3$ were reported in our previous study (Jia et al., 2021).

3. Conclusions and atmospheric implications

In this work, we investigated heterogeneous reactions of NO_2 (~10 ppmv) with K-feldspar, illite, kaolinite, montmorillonite and Arizona Test Dust (ATD) at room temperature as a function of RH (from < 1% to 80%) and reaction time (up to 24 hr), and measured the amounts of nitrate and hygroscopicity before and after NO_2 uptake. Together with our previous studies on heterogeneous reaction of NO_2 with hematite, magnetite, goethite and $CaCO_3$ (Jia et al., 2021; Li et al., 2020), our work provides a comprehensive picture for heterogeneous reaction of NO_2 with mineral dust aerosol.

Heterogeneous reactivity towards NO_2 was found to be very low for illite, kaolinite, montmorillonite and ATD, and the average uptake coefficients of NO_2 in the first 3 hr, $\gamma(NO_2)$, were determined to be around or smaller than 1×10^{-8}. K-feldspar exhibited higher reactivity towards NO_2, and $\gamma(NO_2)$ increased from ~1.5×10^{-8} at <1% RH to ~6.4×10^{-8} at 20%-80% RH; among the nine different types of mineral dust samples we investigated in this and previous work, $CaCO_3$ is most reactive towards NO_2. Overall, our work suggests that mineralogy plays an important role in determining $\gamma(NO_2)$, and $\gamma(NO_2)$ values for minerals investigated in our work can be approximately described by the following order: $CaCO_3$ > K-feldspar > goethite > magnetite > hematite > ATD > three clay minerals (illite, kaolinite, and montmorillonite).

After heterogeneous reaction with 10 ppmv NO_2 for 24 hr, hygroscopicity was not significantly increased for montmorillonite, and increase in hygroscopicity was very small or even insignificant for illite and kaolinite. Small but significant enhancement in hygroscopicity was observed for K-feldspar after heterogeneous reaction with NO_2, and the extent of hygroscopicity enhancement appeared to increase with RH at which NO_2 uptake took place. In addition, large increase in hygroscopicity was observed for ATD after heterogeneous reaction with NO_2, although the increase in hygroscopicity was still

smaller than $CaCO_3$. Therefore, our work shows that not all the mineral dust particles would display enhanced hygroscopicity after heterogeneous reaction with NO_2, and the extent in hygroscopicity enhancement depends critically on mineralogy. It is still not clear why different minerals display different heterogeneous reactivity towards NO_2, and further investigations using surface techniques, such as DRIFTS, may provide mechanistic insights.

Declaration of Competing Interest

The authors declare that they have no known competing financial interests or personal relationships that could have appeared to influence the work reported in this paper.

Acknowledgment

This work was supported by the National Natural Science Foundation of China (No. 42022050), Guangdong Foundation for Program of Science and Technology Research (Nos. 2019B121205006 and 2020B1212060053), the Guangdong Science and Technology Department (No. 2017GC010501) and CAS Pioneer Hundred Talents program.

Appendix A Supplementary data

Supplementary material associated with this article can be found, in the online version, at doi:10.1016/j.jes.2022.07.023.

REFERENCES

Angelini, M.M., Garrard, R.J., Rosen, S.J., Hinrichs, R.Z., 2007. Heterogeneous reactions of gaseous HNO_3 and NO_2 on the clay minerals kaolinite and pyrophyllite. J. Phys. Chem. A 111, 3326–3335.

Chen, L.X.D., Peng, C., Gu, W.J., Fu, H.J., Jian, X., Zhang, H.H., et al., 2020. On mineral dust aerosol hygroscopicity. Atmos. Chem. Phys. 20, 13611–13626.

Creamean, J.M., Suski, K.J., Rosenfeld, D., Cazorla, A., DeMott, P.J., Sullivan, R.C., et al., 2013. Dust and biological aerosols from the sahara and asia influence precipitation in the western U.S. Science 339, 1572–1578.

Crowley, J.N., Ammann, M., Cox, R.A., Hynes, R.G., Jenkin, M.E., Mellouki, A., et al., 2010. Evaluated Kinetic and Photochemical Data for Atmospheric Chemistry: Volume V - Heterogeneous Reactions on Solid Substrates. Atmos. Chem. Phys. 10, 9059–9223.

Denjean, C., Caquineau, S., Desboeufs, K., Laurent, B., Maille, M., Quiñones Rosado, M., et al., 2015. Long-range transport across the Atlantic in summertime does not enhance the hygroscopicity of African mineral dust. Geophys. Res. Lett. 42, 7835–7843.

Dentener, F.J., Carmichael, G.R., Zhang, Y., Lelieveld, J., Crutzen, P.J., 1996. Role of mineral aerosol as a reactive surface in the global troposphere. J. Geophys. Res.-Atmos. 101, 22869–22889.

Dupart, Y., Fine, L., D'Anna, B., George, C., 2014. Heterogeneous uptake of NO_2 on Arizona Test Dust under UV-A irradiation: An aerosol flow tube study. Aeolian Res 15, 45–51.

Ganor, E., Stupp, A., Alpert, P., 2009. A method to determine the effect of mineral dust aerosols on air quality. Atmos. Environ. 43, 5463–5468.

Giannadaki, D., Pozzer, A., Lelieveld, J., 2014. Modeled global effects of airborne desert dust on air quality and premature mortality. Atmos. Chem. Phys. 14, 957–968.

Gibson, E.R., Hudson, P.K., Grassian, V.H., 2006. Physicochemical properties of nitrate aerosols: implications for the atmosphere. J. Phys. Chem. A 110, 11785–11799.

Ginoux, P., Prospero, J.M., Gill, T.E., Hsu, N.C., Zhao, M., 2012. Global-scale attribution of anthropogenic and natural dust sources and their emission rates based on MODIS deep blue aerosol products. Rev. Geophys. 50, RG3005. doi:10.1029/2012RG000388.

Gu, W.J., Li, Y.J., Zhu, J.X., Jia, X.H., Lin, Q.H., Zhang, G.H., et al., 2017. Investigation of water adsorption and hygroscopicity of atmospherically relevant particles using a commercial vapor sorption analyzer. Atmos. Meas. Tech. 10, 3821–3832.

Guo, L.Y., Gu, W.J., Peng, C., Wang, W.G., Li, Y.J., Zong, T.M., et al., 2019. A comprehensive study of hygroscopic properties of calcium- and magnesium-containing salts: implication for hygroscopicity of mineral dust and sea salt aerosols. Atmos. Chem. Phys. 19, 2115–2133.

IUPAC, 2017. IUPAC Task Group on Atmospheric chemical kinetic data evaluation data sheet V.A2.4 MD4, https://iupac-aeris.ipsl.fr/htdocs/datasheets/pdf/Het_MD_NO2_MD4_V.A2.4.pdf. Accessed December 18, 2021.

Jia, X.H., Gu, W.J., Peng, C., Li, R., Chen, L.X.D., Wang, H.L., et al., 2021. Heterogeneous reaction of $CaCO_3$ With NO_2 at different relative Humidities: kinetics, mechanisms, and impacts on aerosol hygroscopicity. J. Geophys. Res.-Atmos. 126. doi:10.1029/2021JD034826, e2021JD034826.

Jickells, T.D., An, Z.S., Andersen, K.K., Baker, A.R., Bergametti, G., Brooks, N., et al., 2005. Global iron connections between desert dust, ocean biogeochemistry, and climate. Science 308, 67–71.

Journet, E., Balkanski, Y., Harrison, S.P., 2014. A new data set of soil mineralogy for dust-cycle modeling. Atmos. Chem. Phys. 14, 3801–3816.

Karydis, V.A., Kumar, P., Barahona, D., Sokolik, I.N., Nenes, A., 2011. On the effect of dust particles on global cloud condensation nuclei and cloud droplet number. J. Geophys. Res.-Atmos. 116, D23204. doi:10.1029/2011JD016283.

Kok, J.F., Ward, D.S., Mahowald, N.M., Evan, A.T., 2018. Global and regional importance of the direct dust-climate feedback. Nat. Commun. 9, 241. doi:10.1038/s41467-017-02620-y.

Krueger, B.J., Grassian, V.H., Cowin, J.P., Laskin, A., 2004. Heterogeneous chemistry of individual mineral dust particles from different dust source regions: the importance of particle mineralogy. Atmos. Environ. 38, 6253–6261.

Krueger, B.J., Grassian, V.H., Laskin, A., Cowin, J.P., 2003. The transformation of solid atmospheric particles into liquid droplets through heterogeneous chemistry: laboratory insights into the processing of calcium containing mineral dust aerosol in the troposphere. Geophys. Res. Lett. 30, 1148. doi:10.1029/2002GL016563.

Laskin, A., Iedema, M.J., Ichkovich, A., Graber, E.R., Taraniuk, I., Rudich, Y., 2005. Direct observation of completely processed calcium carbonate dust particles. Faraday Discuss 130, 453–468.

Li, H.J., Zhu, T., Zhao, D.F., Zhang, Z.F., Chen, Z.M., 2010. Kinetics and mechanisms of heterogeneous reaction of NO_2 on $CaCO_3$ surfaces under dry and wet conditions. Atmos. Chem. Phys. 10, 463–474.

Li, R., Jia, X.H., Wang, F., Ren, Y., Wang, X., Zhang, H.H., et al., 2020. Heterogeneous reaction of NO_2 with hematite, goethite and magnetite: Implications for nitrate formation and iron solubility enhancement. Chemosphere 242, 125273.

Li, W.J., Shao, L.Y., 2009. Observation of nitrate coatings on

atmospheric mineral dust particles. Atmos. Chem. Phys. 9, 1863–1871.
Liu, Y., Han, C., Ma, J., Bao, X., He, H., 2015. Influence of relative humidity on heterogeneous kinetics of NO_2 on kaolin and hematite. Phys. Chem. Chem. Phys. 17, 19424–19431.
Liu, Y.J., Zhu, T., Zhao, D.F., Zhang, Z.F., 2008. Investigation of the hygroscopic properties of $Ca(NO_3)_2$ and internally mixed $Ca(NO_3)_2/CaCO_3$ particles by micro-Raman spectrometry. Atmos. Chem. Phys. 8, 7205–7215.
Ma, Q.X., Liu, Y.C., Liu, C., He, H., 2012. Heterogeneous reaction of acetic acid on MgO, α-Al_2O_3, and $CaCO_3$ and the effect on the hygroscopic behavior of these particles. Phys. Chem. Chem. Phys. 14, 8403–8409.
Mahowald, N.M., Engelstaedter, S., Luo, C., Sealy, A., Artaxo, P., Benitez-Nelson, C., et al., 2009. Atmospheric iron deposition: global distribution, variability, and human perturbations. Ann. Rev. Mar. Sci. 1, 245–278.
Massling, A., Leinert, S., Wiedensohler, A., Covert, D., 2007. Hygroscopic growth of sub-micrometer and one-micrometer aerosol particles measured during ACE-Asia. Atmos. Chem. Phys. 7, 3249–3259.
Matsuki, A., Iwasaka, Y., Shi, G.Y., Zhang, D.Z., Trochkine, D., Yamada, M., et al., 2005. Morphological and chemical modification of mineral dust: Observational insight into the heterogeneous uptake of acidic gases. Geophys. Res. Lett. 32, L22806. doi:10.1029/2005GL024176.
Ndour, M., D'Anna, B., George, C., Ka, O., Balkanski, Y., Kleffmann, J., et al., 2008. Photoenhanced uptake of NO_2 on mineral dust: Laboratory experiments and model simulations. Geophys. Res. Lett. 35, L05812. doi:10.1029/2007GL032006.
Ndour, M., Nicolas, M., D'Anna, B., Ka, O., George, C., 2009. Photoreactivity of NO_2 on mineral dusts originating from different locations of the Sahara desert. Phys. Chem. Chem. Phys. 11, 1312–1319.
Nickovic, S., Vukovic, A., Vujadinovic, M., Djurdjevic, V., Pejanovic, G., 2012. Technical note: high-resolution mineralogical database of dust-productive soils for atmospheric dust modeling. Atmos. Chem. Phys. 12, 845–855.
Prospero, J.M., Mayol-Bracero, O.L., 2013. Understanding the transport and impact of African dust on the caribbean basin. Bull. Amer. Meteorol. Soc. 94, 1329–1337.
Scanza, R.A., Mahowald, N., Ghan, S., Zender, C.S., Kok, J.F., Liu, X., et al., 2015. Modeling dust as component minerals in the community atmosphere model: development of framework and impact on radiative forcing. Atmos. Chem. Phys. 15, 537–561.
Seinfeld, J.H., Pandis, S.N., 2016. Atmospheric Chemistry and Physics: From Air Pollution to Climate Change, Third edition Wiley Interscience, New York.
Shi, Z., Zhang, D., Hayashi, M., Ogata, H., Ji, H., Fujiie, W., 2008. Influences of sulfate and nitrate on the hygroscopic behaviour of coarse dust particles. Atmos. Environ. 42, 822–827.
Shi, Z.B., Krom, M.D., Jickells, T.D., Bonneville, S., Carslaw, K.S., Mihalopoulos, N., et al., 2012. Impacts on iron solubility in the mineral dust by processes in the source region and the atmosphere: a review. Aeolian Res 5, 21–42.
Sullivan, R.C., Guazzotti, S.A., Sodeman, D.A., Prather, K.A., 2007. Direct observations of the atmospheric processing of asian mineral dust. Atmos. Chem. Phys. 7, 1213–1236.
Sullivan, R.C., Moore, M.J.K., Petters, M.D., Kreidenweis, S.M., Roberts, G.C., Prather, K.A., 2009a. Effect of chemical mixing state on the hygroscopicity and cloud nucleation properties of calcium mineral dust particles. Atmos. Chem. Phys. 9, 3303–3316.
Sullivan, R.C., Moore, M.J.K., Petters, M.D., Kreidenweis, S.M., Roberts, G.C., Prather, K.A., 2009b. Timescale for hygroscopic conversion of calcite mineral particles through heterogeneous reaction with nitric acid. Phys. Chem. Chem. Phys. 11, 7826–7837.
Tang, M.J., Cziczo, D.J., Grassian, V.H., 2016. Interactions of water with mineral dust aerosol: water adsorption, hygroscopicity, cloud condensation and ice nucleation. Chem. Rev. 116, 4205–4259.
Tang, M.J., Gu, W.J., Ma, Q.X., Li, Y.J., Zhong, C., Li, S., et al., 2019a. Water adsorption and hygroscopic growth of six anemophilous pollen species: the effect of temperature. Atmos. Chem. Phys. 19, 2247–2258.
Tang, M.J., Huang, X., Lu, K.D., Ge, M.F., Li, Y.J., Cheng, P., et al., 2017. Heterogeneous reactions of mineral dust aerosol: implications for tropospheric oxidation capacity. Atmos. Chem. Phys. 17, 11727–11777.
Tang, M.J., Whitehead, J., Davidson, N.M., Pope, F.D., Alfarra, M.R., McFiggans, G., et al., 2015. Cloud condensation nucleation activities of calcium carbonate and its atmospheric ageing products. Phys. Chem. Chem. Phys. 17, 32194–32203.
Tang, M.J., Zhang, H.H., Gu, W.J., Gao, J., Jian, X., Shi, G.L., et al., 2019b. Hygroscopic properties of saline mineral dust from different regions in China: geographical variations, compositional dependence, and atmospheric implications. J. Geophys. Res.-Atmos 124, 10844–10857.
Textor, C., Schulz, M., Guibert, S., Kinne, S., Balkanski, Y., Bauer, S., et al., 2006. Analysis and quantification of the diversities of aerosol life cycles within AeroCom. Atmos. Chem. Phys. 6, 1777–1813.
Tobo, Y., Zhang, D.Z., Nakata, N., Yamada, M., Ogata, H., Hara, K., et al., 2009. Hygroscopic mineral dust particles as influenced by chlorine chemistry in the marine atmosphere. Geophys. Res. Lett. 36, L05817. doi:10.1029/2008GL036883.
Uno, I., Eguchi, K., Yumimoto, K., Takemura, T., Shimizu, A., Uematsu, M., et al., 2009. Asian dust transported one full circuit around the globe. Nat. Geosci. 2, 557–560.
Usher, C.R., Michel, A.E., Grassian, V.H., 2003. Reactions on mineral dust. Chem. Rev. 103, 4883–4939.
Vlasenko, A., Sjogren, S., Weingartner, E., Stemmler, K., Gaggeler, H.W., Ammann, M., 2006. Effect of humidity on nitric acid uptake to mineral dust aerosol particles. Atmos. Chem. Phys. 6, 2147–2160.
Wu, H.J., Lu, H.Y., Wang, J.J., Chen, Y., Cui, M.C., 2022. A new estimate of global desert area and quantity of dust emission (in Chinese). Chin. Sci. Bull. 67, 860–871.
Yin, Z., Wan, Y., Zhang, Y., Wang, H., 2021. Why super sandstorm 2021 in North China? Natl. Sci. Rev. 9, nwab165. doi:10.1093/nsr/nwab165.
Zhang, R., Jing, J., Tao, J., Hsu, S.C., Wang, G., Cao, J., et al., 2013. Chemical characterization and source apportionment of $PM_{2.5}$ in Beijing: seasonal perspective. Atmos. Chem. Phys. 13, 7053–7074.
Zhang, Z., Shang, J., Zhu, T., Li, H., Zhao, D., Liu, Y., et al., 2012. Heterogeneous reaction of NO_2 on the surface of montmorillonite particles. J. Environ. Sci. 24, 1753–1758.
Zhang, Z.F., Zhu, T., Shang, J., Zhao, D.F., Ye, C.X., 2011. Heterogeneous reaction of NO_2 on the surface of kaolinite particles. Acta Sci. Circumstantiae 31, 2073–2079.